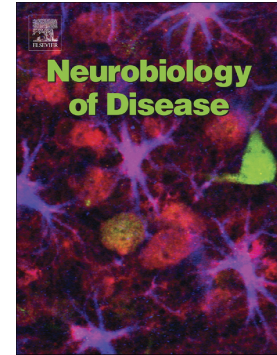


## Accepted Manuscript

Oscillatory neural representations in the sensory thalamus predict neuropathic pain relief by deep brain stimulation

Yongzhi Huang, Alexander L. Green, Jonathan Hyam, James Fitzgerald, Tipu Z. Aziz, Shouyan Wang



PII: S0969-9961(17)30235-8  
DOI: doi:[10.1016/j.nbd.2017.10.009](https://doi.org/10.1016/j.nbd.2017.10.009)  
Reference: YNBDI 4048  
To appear in: *Neurobiology of Disease*  
Received date: 18 July 2017  
Revised date: 25 September 2017  
Accepted date: 11 October 2017

Please cite this article as: Yongzhi Huang, Alexander L. Green, Jonathan Hyam, James Fitzgerald, Tipu Z. Aziz, Shouyan Wang , Oscillatory neural representations in the sensory thalamus predict neuropathic pain relief by deep brain stimulation. The address for the corresponding author was captured as affiliation for all authors. Please check if appropriate. Ynbdi(2017), doi:[10.1016/j.nbd.2017.10.009](https://doi.org/10.1016/j.nbd.2017.10.009)

This is a PDF file of an unedited manuscript that has been accepted for publication. As a service to our customers we are providing this early version of the manuscript. The manuscript will undergo copyediting, typesetting, and review of the resulting proof before it is published in its final form. Please note that during the production process errors may be discovered which could affect the content, and all legal disclaimers that apply to the journal pertain.

---

**Oscillatory neural representations in the sensory thalamus predict  
neuropathic pain relief by deep brain stimulation**

Yongzhi Huang<sup>1,2</sup>, Alexander L. Green<sup>2</sup>, Jonathan Hyam<sup>2</sup>, James Fitzgerald<sup>2</sup>, Tipu Z.

Aziz<sup>2</sup>, Shouyan Wang<sup>1,3\*</sup>

<sup>1</sup> Suzhou Institute of Biomedical Engineering and Technology, Chinese Academy of Sciences,  
Suzhou, 215163, China

<sup>2</sup> Nuffield Department of Surgical Sciences, University of Oxford, John Radcliffe Hospital,  
Oxford, OX3 9DU, UK

<sup>3</sup> Institute of Science and Technology for Brain-inspired Intelligence, Fudan University, Shanghai,  
200433, China

\* Corresponding author. E-mail: shouyan@fudan.edu.cn

## ABSTRACT

*Objective.* Understanding the function of sensory thalamic neural activity is essential for developing and improving interventions for neuropathic pain. However, there is a lack of investigation of the relationship between sensory thalamic oscillations and pain relief in patients with neuropathic pain. This study aims to identify the oscillatory neural characteristics correlated with pain relief induced by deep brain stimulation (DBS), and develop a quantitative model to predict pain relief by integrating characteristic measures of the neural oscillations. *Approach.* Measures of sensory thalamic local field potentials (LFPs) in thirteen patients with neuropathic pain were screened in three dimensional feature space according to the rhythm, balancing, and coupling neural behaviours, and correlated with pain relief. An integrated approach based on principal component analysis (PCA) and multiple regression analysis is proposed to integrate the multiple measures and provide a predictive model. *Main results.* This study reveals distinct thalamic rhythms of theta, alpha, high beta and high gamma oscillations correlating with pain relief. The balancing and coupling measures between these neural oscillations were also significantly correlated with pain relief. *Significance.* The study enriches the series research on the function of thalamic neural oscillations in neuropathic pain and relief, and provides a quantitative approach for predicting pain relief by DBS using thalamic neural oscillations.

**Keywords:** deep brain stimulation; neuropathic pain; local field potentials; neural oscillations

## Introduction

Neuropathic pain is one of the most intractable types of chronic pain. The prevalence of chronic neuropathic pain symptoms in the general population is estimated at 6-8% and it is typically more severe than chronic pain of non-neuropathic origin (Bouhassira et al., 2008; van Hecke et al., 2014). The pathophysiology of neuropathic pain is complicated and involves multiple levels of the nervous system from receptors, ion channels and neurons to neural network systems. Neuropathic pain usually responds poorly to conventional pharmacological treatment. Evidence-based studies have demonstrated that pharmacotherapy for neuropathic pain is far from successful, and fewer than half of patients obtain even partial pain relief (Dworkin et al., 2010; Dworkin et al., 2007; Smith, 2012). Deep brain stimulation (DBS) of the sensory thalamus has been used clinically to relieve neuropathic pain (Hosobuchi et al., 1973; Mazars, 1975; Owen et al., 2006). Such stimulation may prevent pain inputs from activating the pain matrix (Nguyen et al., 2011). However, the efficacy of DBS varies enormously among patients (Hamani et al., 2006; Levy et al., 2010). The mechanism by which stimulation of the thalamus relieves neuropathic pain is not well understood (Boccard et al., 2015).

Direct recordings of local field potentials (LFPs) in patients have been used to study the function of the stimulated nuclei in pain processing. Spindle-shaped neural oscillations of 8–14 Hz have been observed in both the sensory thalamus and the periventricular grey/periaqueductal grey (PVAG). These oscillations correlate with the subjective reporting of pain intensity (Green et al., 2009). In patients with neuropathic

pain, a painful ice-cold stimulus causes a power increase at 17-30 Hz in the sensory thalamus (Green et al., 2009). Neuropathic pain and its relief seems to involve multiple neural oscillations in the thalamus, which can form a local oscillatory network (Priori et al., 2004) and also interact with the PVAG (Wu et al., 2014).

There has been little investigation of the relationship between the oscillatory neural activities in the thalamus and pain relief in patients. It is essential to understand how neural oscillations within different frequency bands are organized as neural assemblies and correlated with pain relief. Such investigation could predict the efficacy of pain relief and enrich the evidence for the potential mechanisms of DBS for the relief of neuropathic pain.

This study aimed to identify the representative neural oscillations related to pain relief induced by DBS, and develop a model to predict the pain relief by integrating characteristic measures of the neural oscillations. The resting LFPs of the sensory thalamus were recorded from patients treated with DBS. The rhythmic, balancing and coupling behaviours of the neural oscillations in LFPs were investigated in three-dimensional feature space: the power of each individual neural oscillation, the power ratio between different oscillations, and the correlative power coupling between multiple oscillations (Huang et al., 2016a). The measures correlating with pain relief were screened using nonlinear regression. Principal component analysis (PCA) was performed to identify the critical component in each dimension, and a multiple variable regression model was formed to predict pain relief based on the critical components of

the thalamic LFPs. The predictability of the model was further verified using the leave-one-out cross-validation approach.

## Methods

The study was approved by the Oxford Research Ethics Committee (OxRec B), and informed written consent was obtained from all patients. All methods of surgical operations, clinical assessment and local field potential recordings were performed according to the guidelines and regulations by NHS Research Ethics Committee.

### Surgical technique

Thirteen patients with chronic neuropathic pain were included in this study (age,  $49 \pm 11$  years; mean  $\pm$  SD) (Supplementary Table S1). All patients underwent unilateral implantation of DBS electrodes into either the sensory thalamus alone or both the sensory thalamus and PVAG at John Radcliffe Hospital, Oxford, UK. The surgical procedures for the targeting and implantation of DBS electrodes (model 3387<sup>TM</sup>, Medtronic<sup>®</sup>, Minneapolis, MN, USA) have been described previously (Bittar et al., 2005a; Boccard et al., 2013; Owen et al., 2006; Wu et al., 2014). In brief, the DBS target structures of the sensory thalamus (VPL/VPM) or PVAG were pre-operatively localized on fused CT/MRI images using Radionics Image Fusion<sup>TM</sup> and Stereoplan<sup>TM</sup> (Radionics, Burlington, MA, USA), and electrode implantation was then performed under local anaesthesia. The electrode placement was targeted to VPM (8-10 mm lateral to the posterior commissure) for face pain and VPL (10-14 mm lateral) for arm and leg pain. Intraoperative test stimulation induced paraesthesia in the area of pain

and dictated the exact electrode placement. The PVAG is targeted 2-3 mm lateral to the posterior commissure and down to the level of the inferior colliculus into the periaqueductal grey area. The somatotopy of this region is inverted such that the feet are at the level of the posterior commissure and face around the inferior colliculus (Bittar et al., 2005b). Intraoperative test stimulation induced a feeling of warmth in the region of pain, dictating the final electrode placement.

The final electrode placement and the localization of each electrode contact were confirmed for all patients on fused images of a post-operative CT scan and pre-operative MRI. In all patients, the DBS electrodes were externalized for one week of trial stimulation to assess the degree of pain relief, and the LFPs were recorded between three and five days after the electrode implantation surgery.

### **Pain assessment**

All patients were asked to rate their pain on a visual analogue scale (VAS) (0-10, where 0 = no pain, 10 = worst pain ever experienced) pain diary twice daily (am and pm) over a period of seven days both before the DBS surgery and within one year after the surgery (Owen et al., 2006; Pereira et al., 2010). In this study, the post-operative VAS assessment was performed between 6 and 12 months after surgery (Boccard et al., 2013). The 14 VAS scores at each time point were averaged to give the mean pain scores at the pre-operative and post-operative stages. The pain relief induced by DBS was computed as the percentage change in the VAS, which was the difference between post- and pre-operative VAS divided by the pre-operative score of each patient.

### **Local field potentials recording**

The LFPs were recorded from the sensory thalamus post-operatively *via* the externalized DBS electrodes. The LFPs were recorded while the patient was unmedicated and before the stimulation was turned on for trial stimulation or after the stimulation was turned off overnight. Bipolar LFPs were recorded from three adjacent pairs of deep brain electrode contacts (contacts 0-1, 1-2, and 2-3) with a common electrode placed on the surface of the mastoid. The recordings were obtained when the patients were seated at rest, and any artefacts were carefully identified and excluded. The LFPs were amplified using isolated CED 1902 amplifiers ( $\times 10\,000$ , Cambridge Electronic Design, Cambridge, UK), filtered between 0.5 Hz and 500 Hz, and digitized using a CED 1401 mark II at a sampling rate of 2000 Hz. The data were displayed on-line and saved on a hard disk using Spike2 (Cambridge Electronic Design, Cambridge, UK).

### **Power spectral density, power ratio and power coupling analysis**

The resting LFPs recorded from the sensory thalamus in 50-s segments were extracted, and recordings from the contacts used for post-operative chronic stimulation were selected for further analysis. The selected LFPs were high-pass filtered at 2 Hz, low-pass filtered at 90 Hz, notch-filtered at 50 Hz, and down-sampled to 500 Hz.

The power spectral density (PSD) was calculated using the Welch periodogram method with a 2-s window and 1-s overlap. To reduce the influence of inter-subject variability, the power spectra were normalized by the integral power between 2 Hz



and 90 Hz. The power within a frequency range was computed as the integral of the PSD over the frequency interval and was denoted as  $R_{(f)}$ , where  $f$  is the central frequency.

The power ratio between two frequencies  $B_{(f_1, f_2)}$  was obtained by calculating the ratio of the power at one frequency  $R_{(f_1)}$  to that at another frequency  $R_{(f_2)}$ . The power ratio analysis characterizes the balance of different thalamic oscillations. In this study, the power was calculated within each 4-Hz frequency bandwidth, and the power ratio matrix was obtained between each frequency pair at every 0.5-Hz step.

To investigate the interaction between different oscillations, the cross-frequency power correlation was computed. The cross-frequency power correlation coupling analysis includes two steps: computation of the time-dependent power in a given frequency band by short-time Fourier transform (STFT) analysis and determination of the cross-correlation between the time-dependent powers of different frequency bands (Bruns and Eckhorn, 2004; Bruns et al., 2000).

The time-frequency representation of the LFPs was obtained by STFT as described in our previous study on the dynamic variation of deep brain LFPs (Wang et al., 2005). In the present study, a 0.25-s Hamming window with a 0.2-s overlap was used to detect rapid changes in LFP activity over time and the transient dynamic modulation between different frequency bands. After obtaining the STFT spectrogram, the time-variant power was computed by averaging the spectrogram over the frequency band of interest. The choice of the bandwidth of the frequency

range influences the result of subsequent power correlation analysis. The bandwidth of the frequency range was defined as 4 Hz. Therefore, the time-variant power was calculated within each 4-Hz frequency band, and the cross-frequency correlation of the time-variant power was obtained between each frequency pair for every 0.5-Hz step. The bandwidth of 4 Hz was selected as a compromise between the time and frequency resolution of STFT. The STFT parameters resulted in a time resolution of 0.25 s and a frequency resolution of ~4 Hz, which are sufficient to detect the  $\delta$ ,  $\theta$ ,  $\alpha$ ,  $\beta$  and  $\gamma$  oscillations.

### Nonlinear regression analysis

The relationship between pain relief and the measures of the thalamic oscillations was quantified with nonlinear regression analysis based on the Boltzmann regression model. The Boltzmann model constrained the range of the pain relief between 0% and 100%, which was properly suitable for the clinical outcome assessment. The Boltzmann models for positive and negative regressions are

$$pain\ relief(\%) = (1 - \frac{1}{1 + e^{(Ind_{LFP} - x)/d}}) \times 100\% \quad \text{and} \quad pain\ relief(\%) = \frac{1}{1 + e^{(Ind_{LFP} - x)/d}} \times 100\% \quad (1)$$

where  $Ind_{LFP}$  is the quantitative measure of the LFPs, for instance, the power at each frequency or the power ratio or power coupling at each frequency pair, and  $x$  and  $d$  are the model parameters to be estimated. The model parameters were estimated iteratively using the Levenberg-Marquardt algorithm, and their statistical significance was tested using the t-test. The statistical significance of the model was tested using the F-test. The correlation between pain relief and the measures was evaluated by

taking the square root of the coefficient of determination. The sign of the correlation coefficient depends on the estimated model (for positive model, positive sign; for negative model, negative sign).

Nonlinear regression analysis was first performed between the power at each frequency and the pain relief, and the procedure was repeated between the power ratio or power coupling at each frequency pair and the pain relief. The frequency ranges and frequency pairs with significant correlations were then identified based on a statistical test for the model with a significance of  $p < 0.01$ . To correct for multiple comparisons, the resulting distributions of  $p$  values were analysed with false discovery rate (FDR) method (Benjamini and Hochberg, 1995). Subsequently, the power, power ratio and power coupling within the identified frequency range or frequency pair were computed again using the power spectral density, power ratio and power coupling analysis. The nonlinear correlations between these LFPs measures and the pain relief were further evaluated using Boltzmann nonlinear regression analysis.

### **Predicting pain relief using PCA and multiple regression analysis**

To predict an individual's pain relief from thalamic LFPs oscillations, the multiple measures were integrated using PCA, and a nonlinear model was developed based on the critical components of the rhythm, balancing and coupling behaviours. First, PCA was applied to each subgroup of the rhythm, balancing and coupling measures. To evaluate the multicollinearity among variables, the correlation among the measures in each subgroup was assessed by multiple Pearson's correlation analysis, and

multicollinearity statistical analysis was performed by computing the variance inflation factor (VIF). Second, Boltzmann nonlinear regression analysis was conducted between the pain relief and the first principal component in each subgroup to obtain three nonlinear regression models. Third, a nonlinear multiple variable prediction model was obtained by performing multiple regression analysis between the pain relief and the three regression models.

The prediction model was further validated using the leave-one-out cross-validation approach. The data from each patient were selected as the test dataset, and the data from the other twelve patients were used as the training dataset to build the model.

The predictive performance of the models was evaluated in terms of the Pearson's correlation between the predicted and actual pain relief, and prediction error.

Supplementary Fig. S1 highlights the modelling procedure of thalamic LFPs for predicting pain relief.

The frequency bands in this paper were defined as  $\delta$  (2-4 Hz),  $\theta$  (4-8 Hz),  $\alpha$  (9-12 Hz), low  $\beta$  (12-20 Hz), high  $\beta$  (20-30 Hz), low  $\gamma$  (30-50Hz), and high  $\gamma$  (50-76 Hz) bands.

The signal processing was conducted using MATLAB (Version 7.1, MathWorks, Inc., Natick, MA, USA), and the statistical analysis was conducted using MATLAB and SPSS (Version 19, IBM, New York, NY, USA).

## Results

### LFPs rhythm characteristics

The patient demographics are detailed in Supplementary Table S1. Pain relief ranged from 4% to 80% (20% (8.5%-52%), median (interquartile range)). The LFPs recorded from the sensory thalamus of patients and the spectra are shown in Fig. 1. The LFPs exhibited oscillatory activity at low and high frequencies, and their spectra exhibited peaks that were particularly prominent in the  $\alpha$  and  $\theta$  bands (Fig. 1C). The power in the  $\alpha$  band in the patient with most significant pain relief (Fig. 1A) was more dominant than that in the patient with least pain relief (Fig. 1B).

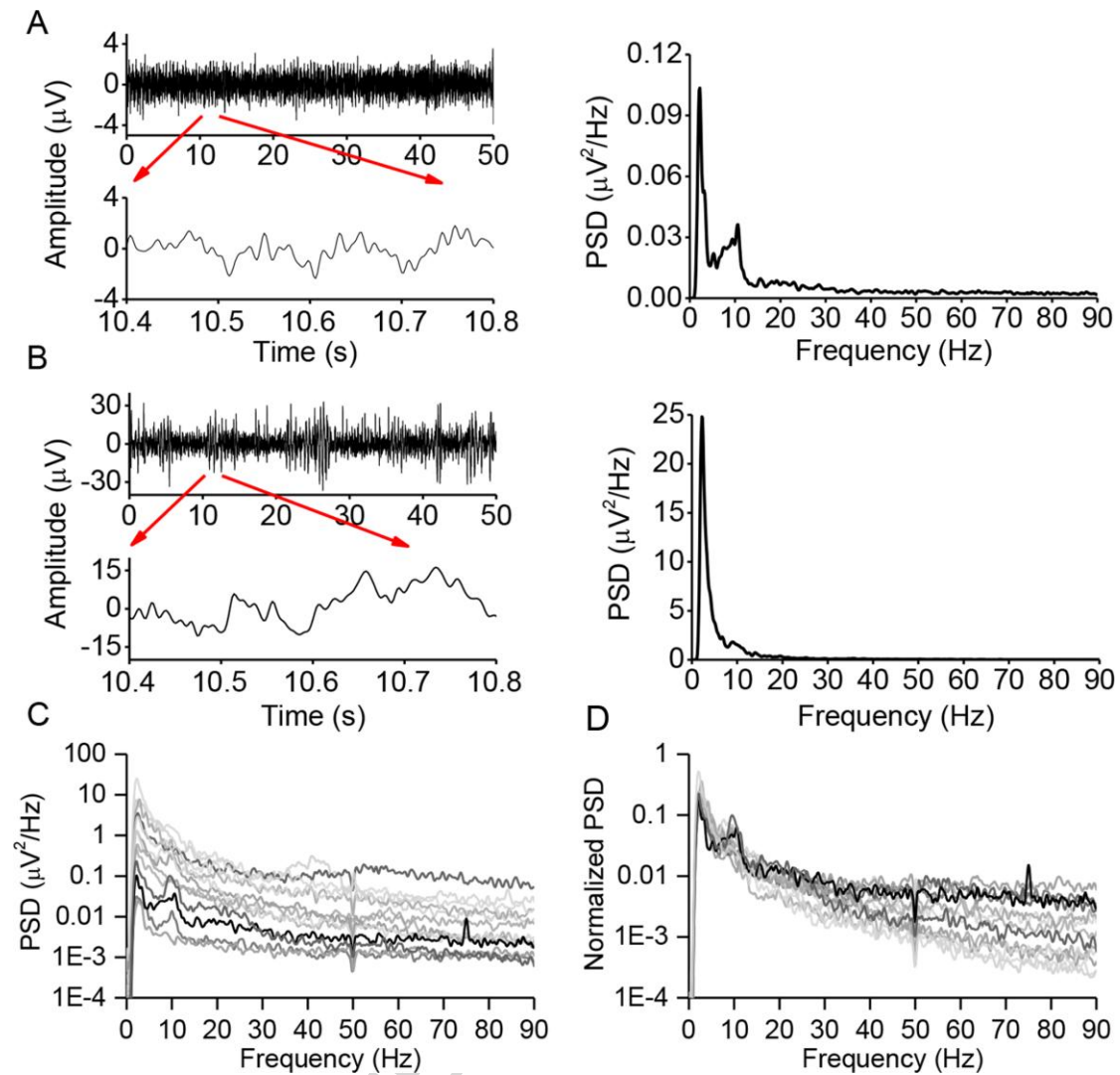


Figure 1. Thalamic LFPs and power spectra from patients with neuropathic pain.

Example of thalamic LFPs and spectra from patients with 80% (A) and 4% pain relief (B). The power spectra of the thalamic LFPs (C) were normalized to the total power in each individual patient (D). The darkness of the lines denotes the pain relief level in each patient, and a darker line indicates greater pain relief (C and D).

### Correlation of pain relief with the power of the thalamic LFPs

The power spectra of the thalamic LFPs were normalized to the total power for each patient, and the averaged spectra are presented (bold line, Fig. 2A). The correlation

between pain relief and the normalized power spectra of the thalamic LFPs at each frequency was evaluated using the nonlinear regression model. The correlation coefficients were computed at each frequency (thin line, Fig. 2A), and the frequency range was marked when the correlation coefficients reached a specified statistical significance level ( $p < 0.01$ , corrected with FDR) (bold coloured line, Fig. 2A). There were four frequency bands with the statistical significance level  $p < 0.01$ : the  $\theta$  (4-8 Hz),  $\alpha$  (9-12 Hz), high  $\beta$  (20-30 Hz) and high  $\gamma$  (50-76 Hz) bands. The power within each frequency band was then calculated and correlated with pain relief. The  $\theta$  power in this range was negatively correlated with pain relief ( $R = -0.61$ ,  $p < 0.01$ , Fig. 2B), and the power in the  $\alpha$ , high  $\beta$  and high  $\gamma$  bands was positively correlated with pain relief ( $R = 0.49$ ,  $p < 0.01$ ;  $R = 0.76$ ,  $p < 0.01$ ;  $R = 0.52$ ,  $p < 0.01$ ; Fig. 2C, D and E, respectively).

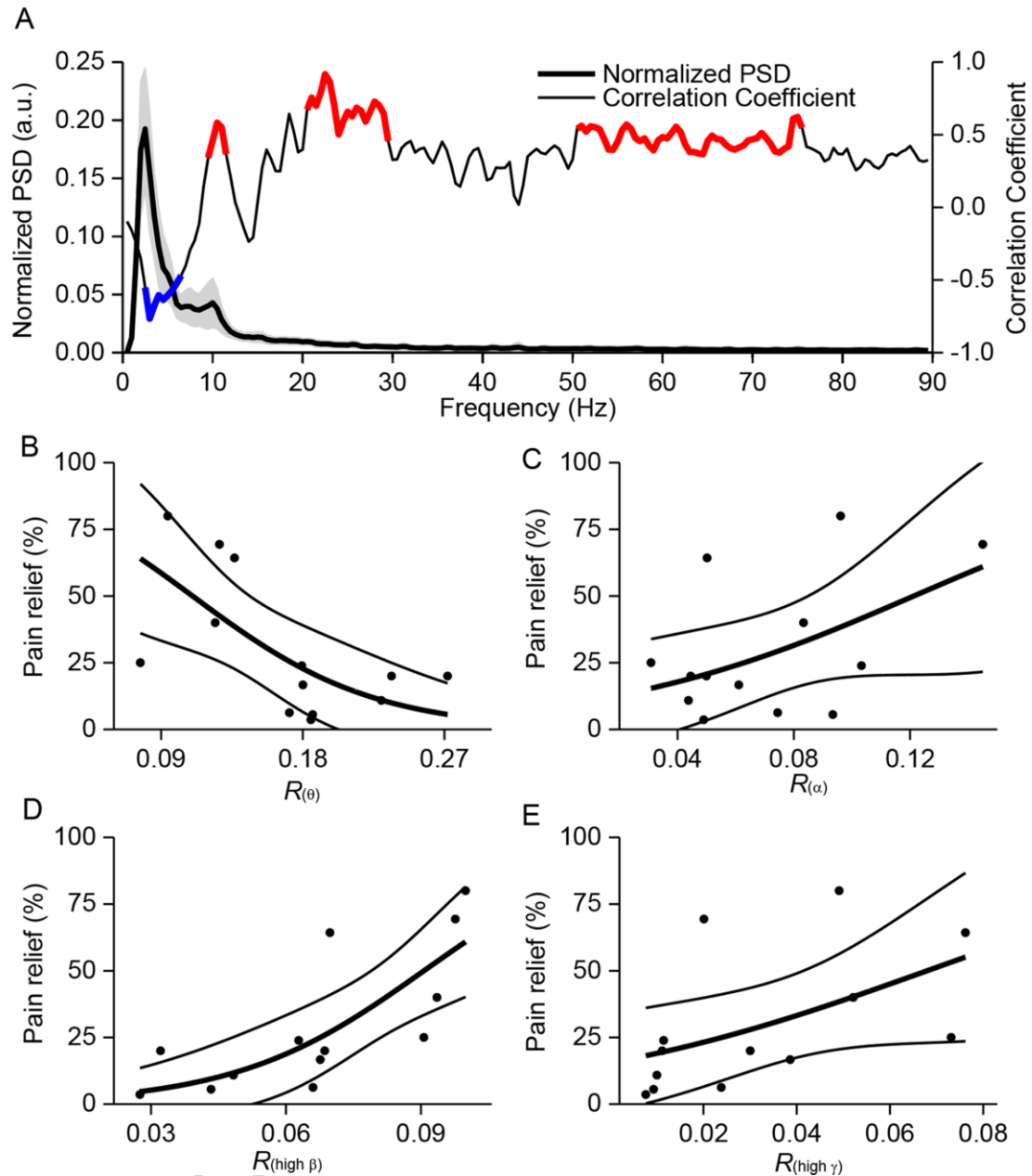


Figure 2. Correlation between pain relief and the rhythm measure in the thalamic LFPs.

Normalized power spectra of thalamic LFPs across all patients (bold line and shadowed region, mean  $\pm$  SD), and correlation coefficients between pain relief and normalized power spectra at each frequency (A). The  $\theta$ ,  $\alpha$ , high  $\beta$  and high  $\gamma$  bands are marked by coloured lines where the negative (blue line) or positive (red line) correlation is statistically significant ( $p < 0.01$ , corrected with FDR). Nonlinear correlation between



pain relief and the powers of  $R_{(\theta)}$  ( $R=-0.61$ ,  $p<0.01$ , B),  $R_{(\alpha)}$  ( $R=0.49$ ,  $p<0.01$ , C),  $R_{(\text{high } \beta)}$  ( $R=0.76$ ,  $p<0.01$ , D) and  $R_{(\text{high } \gamma)}$  ( $R=0.52$ ,  $p<0.01$ , E). The thin lines indicate 95% confidence intervals (B, C, D and E).

### **Correlation of pain relief with power balancing in the thalamic LFPs**

There are multiple neural oscillations correlating to pain perception (Green et al., 2009) and its modulation (Huang et al., 2016b). The organization of these multiple neural oscillations was further investigated in terms of balancing and coupling behaviours. The balancing behaviour was measured as the power ratio between different frequencies, which reflects the relative equilibrium between two neural oscillations. The power ratio was correlated with pain relief using a nonlinear regression model. The power ratio measures averaged over all subjects are presented at each frequency pair (Fig. 3A). The correlation coefficients between pain relief and the power ratio at each frequency pair were calculated (Fig. 3B). The region corresponding to a statistical significance level of  $p<0.01$  (corrected with FDR) was marked. There were four marked rectangular regions:  $(\alpha, \delta + \theta)$ ,  $(\text{high } \beta, \delta)$ ,  $(\text{high } \beta, \text{low } \beta)$ , and  $(\text{high } \gamma, \text{low } \gamma)$ . The frequency ranges for each band were  $\delta$  (2-4 Hz),  $\theta$  (4-8 Hz),  $\alpha$  (9-12 Hz), low  $\beta$  (12-20 Hz), high  $\beta$  (20-30 Hz), low  $\gamma$  (30-50Hz), and high  $\gamma$  (50-76 Hz), and the definition of each ratio was presented in Supplementary Table S2. The power ratio was then calculated within the marked regions in each patient and correlated with the pain relief of the group (Fig. 3C-F). The power ratios  $B_{(\alpha, \delta + \theta)}$ ,  $B_{(\text{high } \beta, \delta)}$ ,  $B_{(\text{high } \beta, \text{low } \beta)}$ , and  $B_{(\text{high } \gamma, \text{low } \gamma)}$  were all positively correlated with pain relief ( $R=0.67$ ,  $p<0.01$ ;

$R=0.72, p<0.01$ ;  $R=0.65, p<0.01$ ;  $R=0.69, p<0.01$ , Fig. 3C-F, respectively). The correlation indicates the contribution of the relative balancing between two neural oscillations to the pain relief.

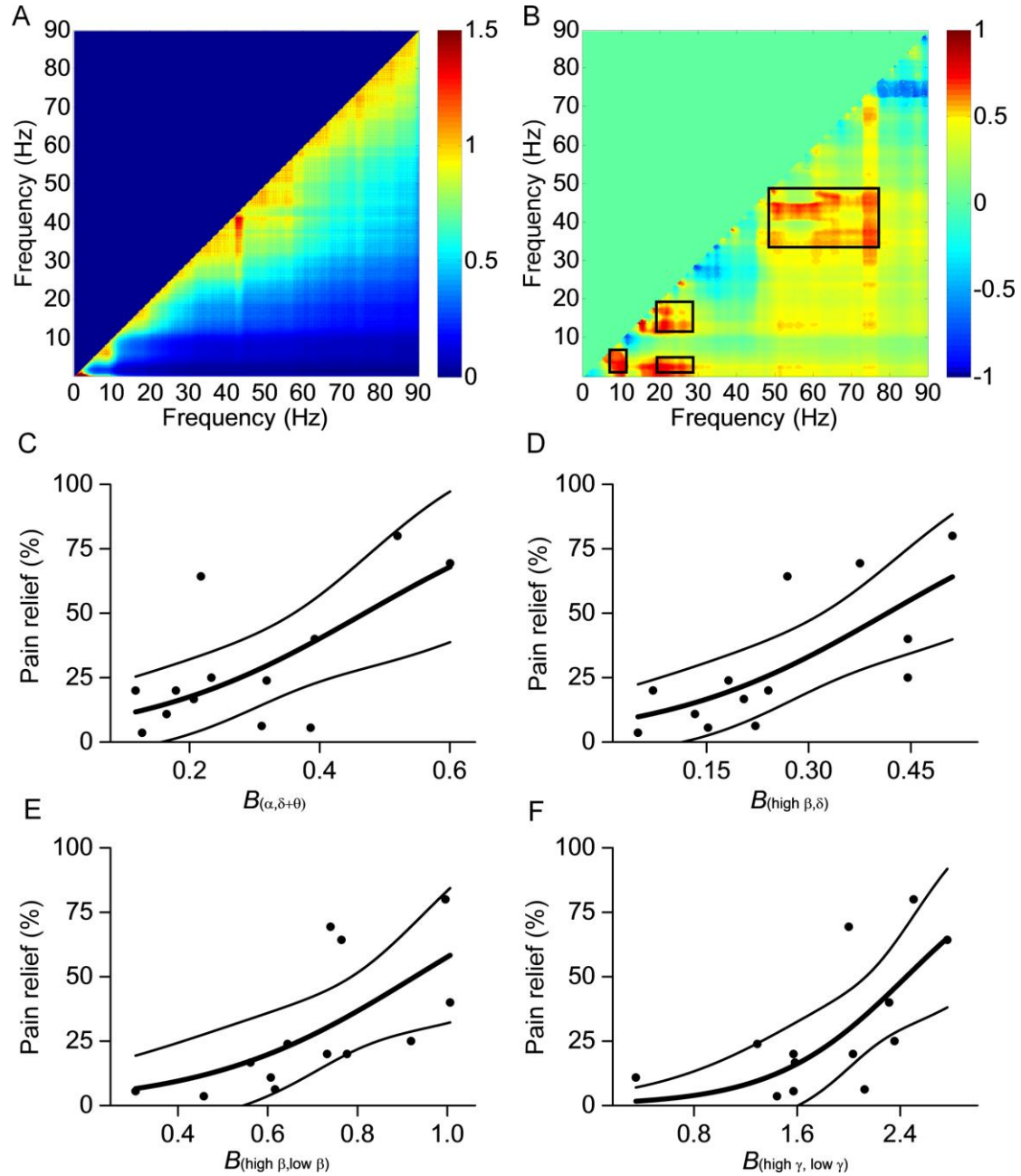


Figure 3. Correlation between pain relief and the balancing measure in the thalamic LFPs. Averaged power ratio matrix between different frequencies across all subjects (A). Correlation coefficients between pain relief and the power ratio of the thalamic

LFPs at each frequency pair (B). The frequency regions are marked by rectangles, within which most of the correlation coefficients are beyond the specified statistical significance level ( $p < 0.01$ , corrected with FDR). Nonlinear correlation between pain relief and the power ratios of  $B_{(\alpha, \delta + \theta)}$  ( $R = 0.67$ ,  $p < 0.01$ , C),  $B_{(\text{high } \beta, \delta)}$  ( $R = 0.72$ ,  $p < 0.01$ , D),  $B_{(\text{high } \beta, \text{low } \beta)}$  ( $R = 0.65$ ,  $p < 0.01$ , E), and  $B_{(\text{high } \gamma, \text{low } \gamma)}$  ( $R = 0.69$ ,  $p < 0.01$ , F). The thin lines indicate 95% confidence intervals (C, D, E and F).

### Correlation of pain relief with power coupling in the thalamic LFPs

The coupling behaviour represents the coherent relationship between neural oscillations, and was measured as the cross-frequency correlation of the time-variant power. The cross-frequency power coupling was computed for each patient, and the averaged power coupling matrix was obtained (Fig. 4A). The correlation between pain relief and the power coupling at each frequency pair was computed across all subjects (Fig. 4B). The frequency regions within which most of the correlation coefficients were beyond the statistical significance level ( $p < 0.01$ , corrected with FDR) was marked (Fig. 4B, the area within the rectangle). There were four marked rectangular regions: (60-70 Hz,  $\delta + \theta$ ), (high  $\beta$ , low  $\beta$ ), (80-90 Hz, 50-60 Hz), and (70-80 Hz, 60-70 Hz), and the definition for each power coupling measure is provided in Supplementary Table S2. The power coupling measures were calculated within the marked regions and correlated with pain relief. Pain relief was positively correlated with  $C_{(60-70 \text{ Hz}, \delta + \theta)}$  ( $R = 0.66$ ,  $p < 0.01$ , Fig. 4C) but negatively correlated with  $C_{(\text{high } \beta, \text{low } \beta)}$  ( $R = -0.65$ ,  $p < 0.01$ , Fig. 4D),  $C_{(80-90 \text{ Hz}, 50-60 \text{ Hz})}$  ( $R = -0.65$ ,  $p < 0.01$ , Fig. 4E), and  $C_{(70-80 \text{ Hz}, 60-70 \text{ Hz})}$  ( $R = -0.75$ ,  $p < 0.01$ , Fig. 4F). The correlation indicates the contribution of the

interaction between neural oscillations to the pain relief.

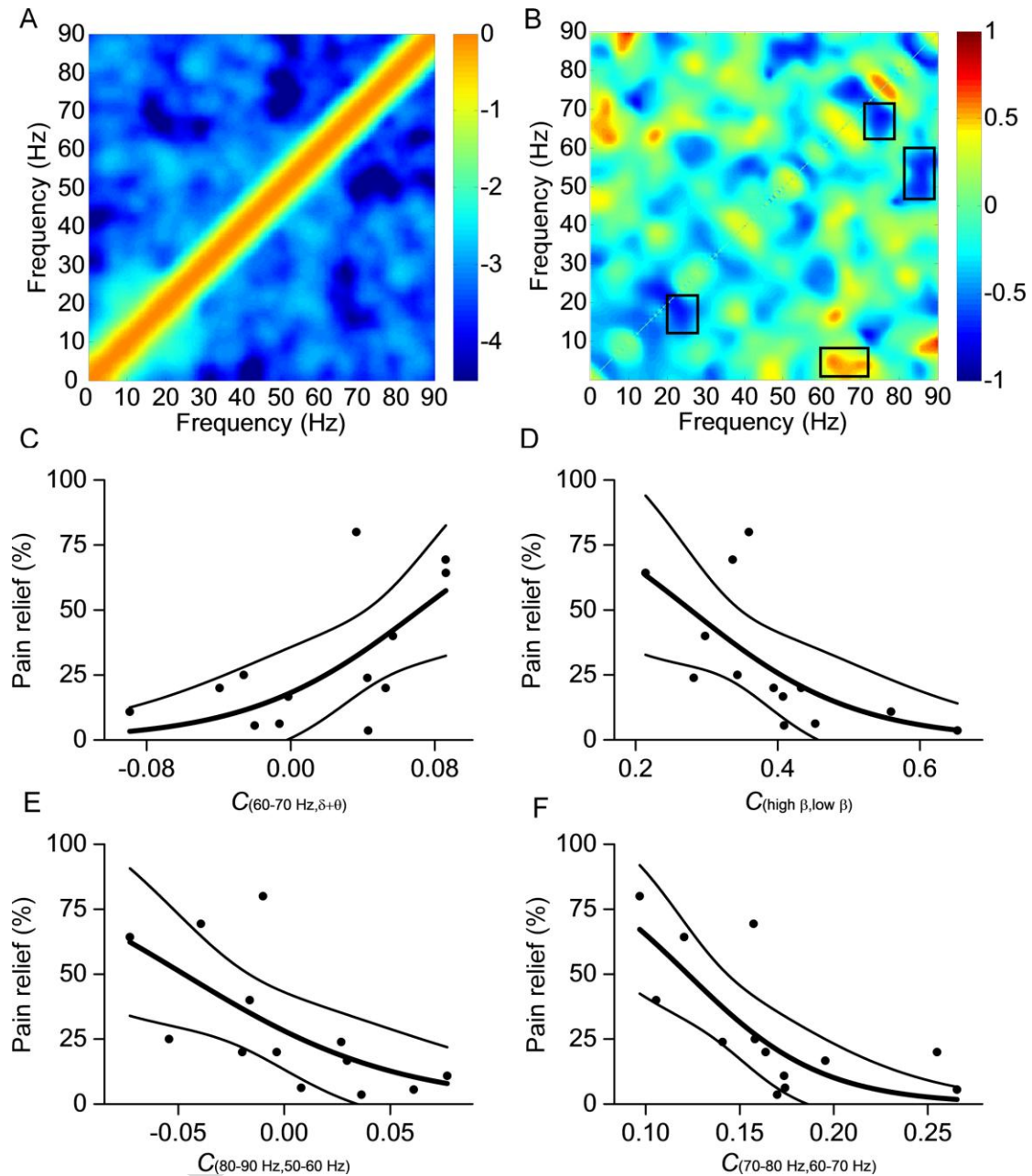


Figure 4. Correlation between pain relief and the coupling measure in the thalamic LFPs. Average power coupling matrix between different frequencies across all patients (A). Note that the values shown in the figure are the natural log ( $\ln$ ) of the power coupling measures. Correlation coefficients between pain relief and the power coupling measure of the thalamic LFPs at each frequency pair (B). The frequency

regions within which most of the correlation coefficients are beyond the specified statistical significance level ( $p < 0.01$ ) are marked by rectangles. Nonlinear correlation between pain relief and the power coupling of  $C_{(60-70 \text{ Hz}, \delta + \theta)}$  ( $R = 0.66$ ,  $p < 0.01$ , C),  $C_{(\text{high } \beta, \text{ low } \beta)}$  ( $R = -0.65$ ,  $p < 0.01$ , D),  $C_{(80-90 \text{ Hz}, 50-60 \text{ Hz})}$  ( $R = -0.65$ ,  $p < 0.01$ , E), and  $C_{(70-80 \text{ Hz}, 60-70 \text{ Hz})}$  ( $R = -0.75$ ,  $p < 0.01$ , F). The thin lines indicate 95% confidence intervals (C, D, E and F).

### **Integration of multiple neural rhythm, balancing, and coupling measures in thalamic LFPs**

There were multiple measures in each of the neural rhythm, balancing and coupling subgroups. To reduce the redundancy of the multiple measures, PCA and multiple variable regression were applied. Integration processing of the multiple measures further improved the correlation between the neural measures and the pain relief.

The multiple correlation analysis and VIF values confirmed the multicollinearity between the measures in each group (Supplementary Tables S3, S4 and S5). PCA was applied to the measures in each subgroup. For the rhythm measures, the first principal component accounted for 72% of the variance of the data. Moreover, the first principal component was more strongly correlated with pain relief than any individual measures ( $R = 0.77$ ,  $p < 0.01$ , Fig. 5A). For the balancing measures, the first principal component accounted for 78% of the variance of the data, and the correlation with pain relief was stronger than that of any individual measure ( $R = 0.81$ ,  $p < 0.01$ , Fig. 5B). For the coupling measures, the first principal component accounted for 71% of

the variance of the data and was also more strongly correlated with pain relief

( $R=0.84$ ,  $p<0.01$ , Fig. 5C).

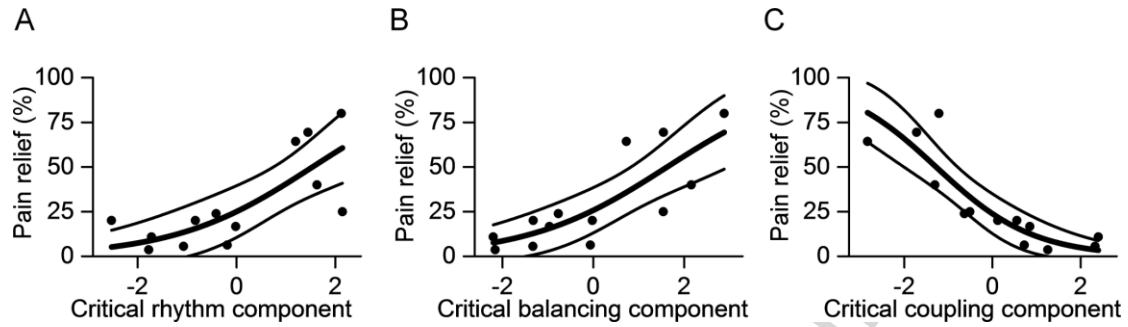


Figure 5. Nonlinear correlation between pain relief and the critical components in the rhythm, balancing and coupling measures ( $R=0.77$ ,  $p<0.01$ ,  $R=0.81$ ,  $p<0.01$ ,  $R=0.84$ ,  $p<0.01$ , respectively, A, B and C). Thin lines indicate 95% confidence intervals (A, B and C).

### Prediction of pain relief with the nonlinear multi-variate model of the integrative measures

The nonlinear regression model between pain relief and the first principal component in each subgroup was estimated. Then, multiple regression analysis was performed using these nonlinear regression models. The prediction model was

$$V_{predict} = a_0 + a_1 \left( 100 - \frac{100}{1 + e^{(R - M_R)/d_R}} \right) + a_2 \left( 100 - \frac{100}{1 + e^{(B - M_B)/d_B}} \right) + a_3 \left( \frac{100}{1 + e^{(C - M_C)/d_C}} \right) \quad (2)$$

where  $V_{predict}$  is the predicted pain relief and  $R$ ,  $B$  and  $C$  are the first principal components in the rhythm, balancing and coupling subgroups, respectively.  $M_R$  and  $d_R$  are the model parameters in the rhythm measures,  $M_B$  and  $d_B$  are the model parameters in the balancing measures, and  $M_C$  and  $d_C$  are the model parameters in the coupling measures. These parameters were obtained from the nonlinear regression

analysis between the pain relief and the first principal component in each subgroup.

$a_0$ ,  $a_1$ ,  $a_2$  and  $a_3$  are the regression coefficients of the prediction model. The regression coefficients were estimated using multiple regression analysis between the pain relief and the three nonlinear regression models with the data from thirteen patients, and the coefficient of determination of the regression model  $R^2$  was 0.81 ( $p < 0.01$ ), indicating that these critical principal components fit the prediction model well.

The performance of the prediction model was verified using the leave-one-out cross-validation approach, i.e., the measures from one patient were selected as the test data set, and the others were used to compute the prediction model. Pearson's correlation between the predicted and actual pain reliefs was 0.85 (Fig. 6B), and the prediction error was  $10.5 \pm 8.2\%$  (Fig. 6C). The predicted VAS of the post-operative pain assessment was then compared with the actual VAS. Pearson's correlation between the predicted and actual post-operative VAS was 0.89 (Fig. 6B), and the prediction error of the post-operative VAS score was  $0.9 \pm 0.7$  (Fig. 6C). The prediction performed better when the post-operative pain level was higher and there was less pain relief (Fig. 6A). The performances of the regression models based on the rhythm measure, balancing measure, and coupling measure were verified as well. Pearson's correlations between the predicted and actual pain relief using these three measures were 0.61, 0.70, and 0.76, respectively (Fig. 6B), and the prediction errors were  $16.0 \pm 13.0\%$ ,  $14.5 \pm 10.8\%$ , and  $12.7 \pm 11.3\%$ , respectively (Fig. 6C). Pearson's correlations between the predicted and actual post-operative VAS were 0.74, 0.83, and

0.82, respectively (Fig. 6B), and the prediction errors of the post-operative VAS scores were  $1.3 \pm 1.1$ ,  $1.1 \pm 0.8$ , and  $1.0 \pm 1.1$ , respectively (Fig. 6C). These results indicate that the prediction approach integrating rhythm, balancing and coupling measures provided the best performance, as evidenced by the higher correlation (Fig. 6B) and lower values of the mean and variation of the prediction error (Fig. 6C).

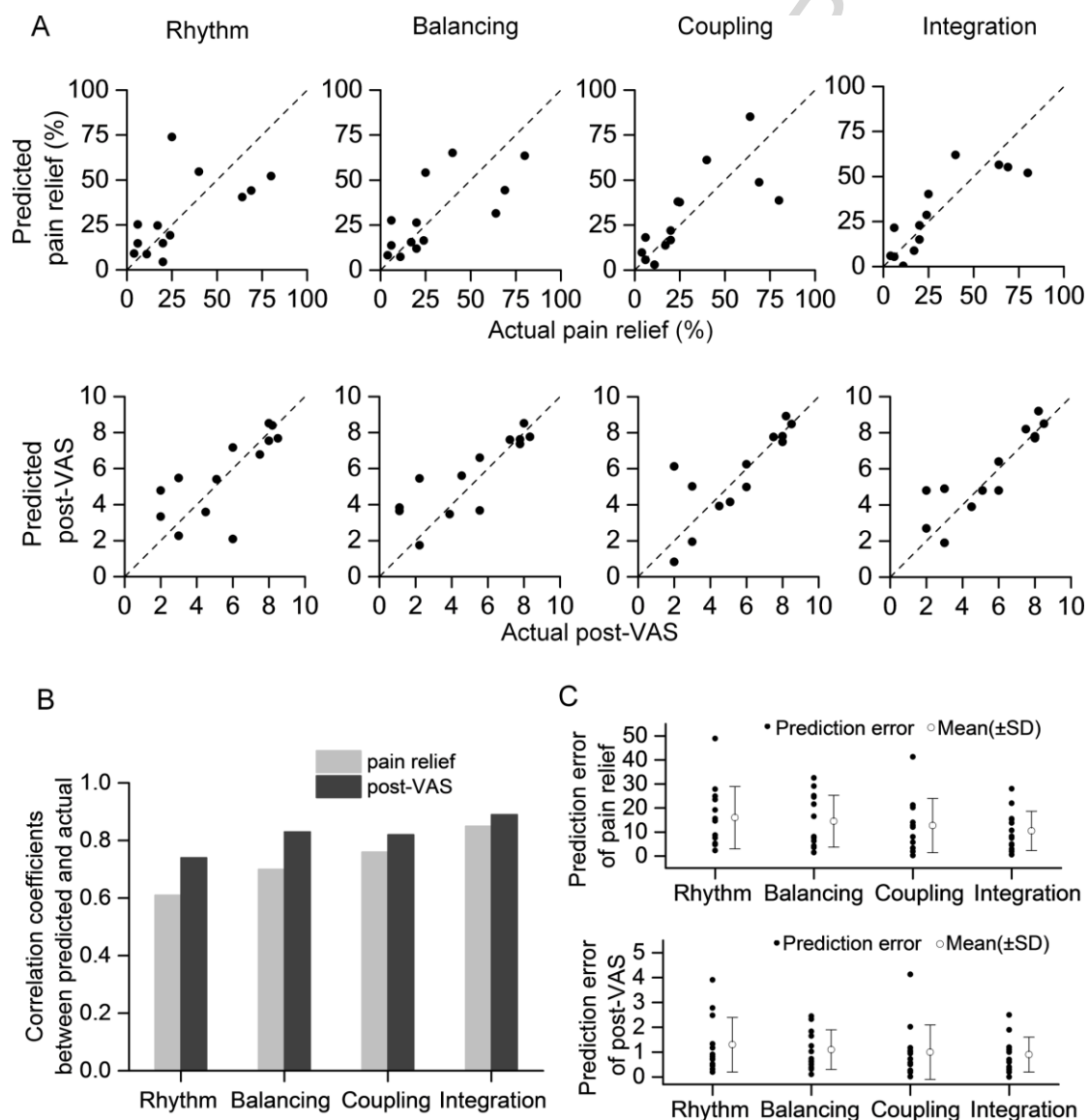


Figure 6. Correlation between the predicted and actual pain relief and between the predicted and actual post-operative VAS using the rhythm model, balancing model, coupling model and integration prediction model (A). Pearson's correlation



coefficients between the predicted and actual pain relief, between the predicted and actual post-operative VAS using these models (B), and the prediction errors (C).

## Discussion

This study demonstrates that pain relief associated with DBS is related to multiple neural oscillations coherently.

There is little research on neurophysiological function in the deep brain related to pain relief provided by DBS in patients with neuropathic pain (Pereira and Aziz, 2014).

Challenges include high variability among individuals and the fact that there is no objective measure of pain. In this study, LFPs from the sensory thalamus were analysed to quantitatively predict pain relief induced by DBS. The prediction approach integrated rich neural information, and was critically validated. Firstly, the representative measures of the neural oscillations were thoroughly screened in three dimensions according to the rhythm, balancing, and coupling neural behaviours in the sensory thalamic LFPs. The measures significantly correlated with pain relief were statistically assessed with FDR correction. Then, the critical components in each dimension were extracted using PCA. A nonlinear prediction model was developed by combining the three critical components. The performance of the prediction model was verified using the leave-one-out approach, and the predicted and actual post-operative VAS achieved a correlation coefficient of 0.89. The performance in predicting pain relief was improved by the two-stage of segregation and integration process.

We found that the theta, alpha, beta and gamma oscillations were related to pain relief with DBS. Neuropathic pain is known to modulate brain oscillations in humans and animals. Evidence from human studies has suggested that altered thalamic burst firing and thalamocortical dysrhythmia play a crucial role in neuropathic pain (Gorecki et al., 1989; Jones, 2010; Lenz et al., 1989; Sarnthein and Jeanmonod, 2008; Sarnthein et al., 2006). Low-frequency bursting has been recorded from single neurons in the thalamus of patients with neurogenic pain (Jeanmonod et al., 1996, 1993; Lenz et al., 1989; Rinaldi et al., 1991). Thalamic neurons hyperpolarize sufficiently to deactivate calcium channels, resulting in the production of low-threshold calcium-spike bursts (Lenz et al., 1989). The threshold calcium-spike bursts have been found to appear as rhythmic bursting activity with an average inter-burst interval of  $263 \pm 46$  ms (Jeanmonod et al., 1996). Such a burst discharge is proposed to correlate with the delta and theta oscillations in thalamic LFPs. Thalamic relay neurons are thought to influence thalamocortical loops, particularly in the theta frequency range, which may underlie the pathophysiology of neuropathic pain (Llinas et al., 1999; Sarnthein et al., 2006). Excessive theta thalamic activity is regarded as a trigger for cortical dysfunction resulting in thalamocortical dysrhythmia (Llinas et al., 1999; Sarnthein et al., 2006). Such altered thalamic activity has also been observed in animal models with neuropathic pain (Gerke et al., 2003; Hains et al., 2006). Recent animal studies showed that chronic neuropathic pain attenuates signal coherence of thalamocortical oscillations in the low-frequency (2 to 30 Hz) range, while enhancing theta power amplitude in the cortex (LeBlanc et al., 2016a; Leblanc et al., 2014). A follow-up

study suggested that pain-induced cortical synchrony and thalamocortical disconnectivity are directly related to burst firing in VPL thalamus (LeBlanc et al., 2016b). Moreover, a further study using optogenetic strategies for selective modulation of the thalamocortical network showed that optically-induced thalamic bursts attenuate cortical theta and mechanical allodynia (LeBlanc et al., 2017), also suggesting that thalamus bursts play a key role in regulating cortical theta and nociceptive behaviour. In the current study, we have found significant correlations between pain relief and the synchronization level of theta, alpha, high beta and high gamma oscillations. There is some evidence that theta oscillation in the thalamus can be suppressed by PVAG stimulation at useful frequencies (Wu et al., 2014). The thalamic alpha and beta oscillations were proposed as the underlying biomarkers closely related to subjective pain perception (Green et al., 2009; Zhang et al., 2013). Gamma band activity has been observed in many cortical areas and in subcortical structures, but its functional significance remains unclear. Several studies have implicated gamma rhythms in pain (Llinas et al., 1999; Schulz et al., 2012). Increased thalamic gamma band activity is observed during painful cutaneous laser stimulation (Kim et al., 2015), whereas anaesthesia with propofol decreases thalamic high-gamma power (Verdonck et al., 2014). However, the relationship between thalamic gamma band activity and pain relief in patients with neuropathic pain has not been studied. Our results suggest that gamma band power predicts pain relief, indicating the functional role of thalamic gamma rhythms in pain.

Pain perception and modulation might be related to the integrative and coherent

contribution from multiple neural oscillations (Huang et al., 2016b; Ray et al., 2009; Sarnthein et al., 2003). It has been found that the power ratios between theta and alpha, and theta and beta bands in the Electroencephalogram (EEG) significantly contribute to attention (Barry et al., 2003; Bresnahan et al., 1999; Putman et al., 2010), and power ratio between delta and alpha bands has been shown to be related to the occurrence of fibromyalgia (Rosenfeld et al., 2015) and chronic pain (Della Marca et al., 2013). Significant phase and power coupling between theta and beta thalamic oscillations has been observed in patients with neurogenic pain and is considered a key element for understanding thalamocortical dysrhythmias (Sarnthein et al., 2003). The integrative measures between different thalamic neural oscillations were more predictive of pain relief. For example, the regression models based on the balancing measure and coupling measure provided a prediction with correlation coefficient values of 0.70 and 0.76, respectively. This was further improved by using the rhythm measure (0.61). The best prediction, moreover, combined the three measures giving a correlation coefficient of 0.85. These studies indicate the importance of the relationship between oscillations in neuropathic pain and its relief, not just individual rhythms, and these multiple oscillations measures might be involved in the pathophysiology of pain, which could be further investigated by simultaneous recordings of single units, LFPs, and/or EEG in patients with neuropathic pain, enabling us to examine neural dynamics and thalamocortical circuit related to pain at multiple spatial scales. Further study could also investigate the direct relationships between these measures and pain by recording the LFPs in single patients for a long

period of time and assessing the pain intensity simultaneously, which would enable us to see the dynamic changes in the measures in neuronal oscillations in different pain state. Moreover, the LFPs could be recorded while cycling the patient on and off a pain relieving train of DBS stimulation to evaluate the effects of DBS on the measures in neuronal oscillations.

The effectiveness of deep brain stimulation for alleviating certain cases of phantom limb pain may involve depolarization of thalamocortical dysrhythmias, which would interrupt low frequency oscillations (Ray et al., 2009). Reduced correlations between frequencies have also been found after stimulation compared with before stimulation, suggesting that DBS might interfere with cross-frequency neural interaction when alleviating pain (Ray et al., 2009). Although the underlying mechanism remains unclear, the correlation between pain relief and power balancing and coupling between different frequencies suggests that these behaviours may be used as a quantifiable biomarker for pain modulation.

The current study may advance the strategy of deep brain stimulation towards modulating the balancing and coupling of neural oscillations. In Parkinson's disease, DBS suppresses the over-synchronized beta oscillations (Kühn et al., 2008), and adaptive stimulation according to the level of beta synchronization achieves a superior performance to continuous stimulation (Little et al., 2013). In neuropathic pain, the suppression of theta oscillations might be related to effective treatment (Wu et al., 2014). It is possible that high or low frequency stimulation may be optimized according to the balancing between different frequency bands of neural oscillations,

i.e. dynamically adjusted according to such objective measures (Udupa and Chen, 2015). Such adaptive stimulation strategy could improve the performance of deep brain stimulation for neuropathic pain by intermittently exciting or inhibiting two neural oscillations rather than only modulating single one with fixed frequency stimulation. The reliable dynamic identification of these multiple measures will further advance the translation of current findings to the development of the closed-loop stimulation for neuropathic pain. The precisely selective modulation of individual feature could be achieved by developing adaptive control models with multiple inputs and outputs, or temporally identifying and modulating the occurrence of each feature. Our recent preliminary study has established a state identification method to dynamically identify the synchronization and de-synchronization states of neural oscillations in pain (Luo et al., 2017). The development of reliable dynamic neural state coding for pain by integrating the measures of multiple neural oscillations will advance adaptive neural stimulation techniques.

There are some noteworthy limitations of this study. The sample size was small, and there was large variation in pain relief between subjects. This large variation, however, provides an opportunity to investigate the relationship between extremes in effect of DBS. Both signal processing and statistical approaches were integrated to critically validate the significance of the regression and prediction to assure the reliability of the approaches. There might remain insertional effects influencing the neural activities although the LFPs recording in this study was made between 3-5 days after the implantation and the effects are likely to have worn off. The immediate effects after

the implantation could cause mechanical injury and focal edema (Haberler et al., 2000), and such insertional influence reduces in a few days (Benabid et al., 1996; Tasker, 1998). Long-term effects due to gliosis or tissue reaction could last from several days to months. The LFPs recorded pre- /post-operatively have provided valuable information to reveal the neurophysiological and neuropathological functions of the nucleus (Brittain and Brown, 2014; Friston et al., 2015; Jenkinson and Brown, 2011). Furthermore, DBS electrodes were implanted in both sensory thalamus and PVAG in most patients. This indicates that the pain relief could be the combined effect from two nuclei rather than the single effect from the sensory thalamus. Both sensory thalamus and PVAG correlated to the pain modulation. Although we cannot distinguish the component of pain relief contributed by each nucleus, the current study elucidated the relationships between the neural oscillations in the sensory thalamus and the overall pain relief induced by DBS. It demonstrated the potential links between the neural oscillations and pain relief induced by multiple factors. Further works are needed to determine the effects of sensory thalamus and PVAG respectively by using more selective approaches, for instance, optogenetic modulation (LeBlanc et al., 2017).

Finally, the accuracy of electrode location is a potential confound that is relevant to both the characteristics of neural activity and the therapy response. In the current study, the location of selected contacts were verified by the imaging, testing stimulation and pain relief performance. We believe that this is adequate to determine accuracy within a few mm. However, as the sensory thalamus is not easily definable

on imaging, one possible improvement would be to measure sensory thresholds to provide objective information to confirm the position of each electrode contact and this would be recommended in the future.

## **Conclusion**

This study identifies the characteristics in sensory thalamic neural oscillations related to pain relief, and provides a model for predicting the outcomes of neuropathic pain relief by DBS.

## **Acknowledgements**

The authors declare no competing financial interests. We thank Professor Peter Brown for constructive and critical comments. Shouyan Wang is supported by the National Natural Science Foundation of China (81471745), the Suzhou Key Laboratory of Neural Engineering and Technology (SZS01414), and the Suzhou Medical Device and Medicine Key Program (ZXY201425). Alexander L. Green, James Fitzgerald and Tipu Z. Aziz are supported by the Oxford NIHR Biomedical Research Centre.



## References

- Barry RJ, Clarke AR, Johnstone SJ. A review of electrophysiology in attention-deficit/hyperactivity disorder: I. Qualitative and quantitative electroencephalography. *Clin Neurophysiol*, 2003; 114: 171-83.
- Benabid AL, Pollak P, Gao DM, Hoffmann D, Limousin P, Gay E, Payen I, Benazzouz A. Chronic electrical stimulation of the ventralis intermedius nucleus of the thalamus as a treatment of movement disorders. *J Neurosurg*, 1996; 84: 203-14.
- Benjamini Y, Hochberg Y. Controlling the false discovery rate: a practical and powerful approach to multiple testing. *Journal of the Royal Statistical Society. Series B (Methodological)*, 1995: 289-300.
- Bittar RG, Kar-Purkayastha I, Owen SL, Bear RE, Green A, Wang S, Aziz TZ. Deep brain stimulation for pain relief: a meta-analysis. *J Clin Neurosci*, 2005a; 12: 515-9.
- Bittar RG, Nandi D, Carter H, Aziz TZ. Somatotopic organization of the human periventricular gray matter. *J Clin Neurosci*, 2005b; 12: 240-1.
- Boccard SG, Pereira EA, Aziz TZ. Deep brain stimulation for chronic pain. *J Clin Neurosci*, 2015; 22: 1537-43.
- Boccard SGJ, Pereira EAC, Moir L, Aziz TZ, Green AL. Long-term outcomes of deep brain stimulation for neuropathic pain. *Neurosurgery*, 2013; 72: 221-30.
- Bouhassira D, Lanteri-Minet M, Attal N, Laurent B, Touboul C. Prevalence of chronic

pain with neuropathic characteristics in the general population. *Pain*, 2008; 136: 380-7.

Bresnahan SM, Anderson JW, Barry RJ. Age-related changes in quantitative EEG in attention-deficit/hyperactivity disorder. *Biol Psychiatry*, 1999; 46: 1690-7.

Brittain JS, Brown P. Oscillations and the basal ganglia: Motor control and beyond. *Neuroimage*, 2014; 85: 637-47.

Bruns A, Eckhorn R. Task-related coupling from high- to low-frequency signals among visual cortical areas in human subdural recordings. *Int J Psychophysiol*, 2004; 51: 97-116.

Bruns A, Eckhorn R, Jokeit H, Ebner A. Amplitude envelope correlation detects coupling among incoherent brain signals. *Neuroreport*, 2000; 11: 1509-14.

Della Marca G, Frusciante R, Vollono C, Iannaccone E, Dittoni S, Losurdo A, Testani E, Gnani V, Colicchio S, Di Blasi C. Pain and the alpha- sleep anomaly: A mechanism of sleep disruption in facioscapulohumeral muscular dystrophy. *Pain Med*, 2013; 14: 487-97.

Dworkin RH, O'Connor AB, Audette J, Baron R, Gourlay GK, Haanpaa ML, Kent JL, Krane EJ, Lebel AA, Levy RM, Mackey SC, Mayer J, Miaskowski C, Raja SN, Rice AS, Schmader KE, Stacey B, Stanos S, Treede RD, Turk DC, Walco GA, Wells CD. Recommendations for the pharmacological management of neuropathic pain: an overview and literature update. *Mayo Clin Proc*, 2010; 85: S3-14.

Dworkin RH, O'Connor AB, Backonja M, Farrar JT, Finnerup NB, Jensen TS, Kalso EA, Loeser JD, Miaskowski C, Nurmikko TJ, Portenoy RK, Rice AS, Stacey BR, Treede RD, Turk DC, Wallace MS. Pharmacologic management of neuropathic pain: evidence-based recommendations. *Pain*, 2007; 132: 237-51.

Friston KJ, Bastos AM, Pinotsis D, Litvak V. LFP and oscillations - what do they tell us? *Curr Opin Neurobiol*, 2015; 31: 1-6.

Gerke M, Duggan A, Xu L, Siddall P. Thalamic neuronal activity in rats with mechanical allodynia following contusive spinal cord injury. *Neuroscience*, 2003; 117: 715-22.

Gorecki J, Hirayama T, Dostrovsky J, Tasker R, Lenz F. Thalamic stimulation and recording in patients with deafferentation and central pain. *Stereotact Funct Neurosurg*, 1989; 52: 219-26.

Green AL, Wang S, Stein JF, Pereira EAC, Kringelbach ML, Liu X, Brittain JS, Aziz TZ. Neural signatures in patients with neuropathic pain. *Neurology*, 2009; 72: 569-71.

Haberler C, Alesch F, Mazal PR, Pilz P, Jellinger K, Pinter MM, Hainfellner JA, Budka H. No tissue damage by chronic deep brain stimulation in Parkinson's disease. *Ann Neurol*, 2000; 48: 372-6.

Hains BC, Saab CY, Waxman SG. Alterations in burst firing of thalamic VPL neurons and reversal by Nav1.3 antisense after spinal cord injury. *J Neurophysiol*, 2006; 95: 3343-52.

Hamani C, Schwalb JM, Rezai AR, Dostrovsky JO, Davis KD, Lozano AM. Deep brain stimulation for chronic neuropathic pain: Long-term outcome and the incidence of insertional effect. *Pain*, 2006; 125: 188-96.

Hosobuchi Y, Adams JE, Rutkin B. Chronic thalamic stimulation for the control of facial anesthesia dolorosa. *Arch Neurol*, 1973; 29: 158-61.

Huang Y, Geng X, Li L, Stein JF, Aziz TZ, Green AL, Wang S. Measuring complex behaviors of local oscillatory networks in deep brain local field potentials. *J Neurosci Methods*, 2016a; 264: 25-32.

Huang Y, Luo H, Green AL, Aziz TZ, Wang S. Characteristics of local field potentials correlate with pain relief by deep brain stimulation. *Clin Neurophysiol*, 2016b; 127: 2573-80.

Jeanmonod D, Magnin M, Morel A. Low-threshold calcium spike bursts in the human thalamus - common physiopathology for sensory, motor and limbic positive symptoms. *Brain*, 1996; 119: 363-75.

Jeanmonod D, Magnin M, Morel A. Thalamus and neurogenic pain - physiological, anatomical and clinical-data. *Neuroreport*, 1993; 4: 475-8.

Jenkinson N, Brown P. New insights into the relationship between dopamine, beta oscillations and motor function. *Trends Neurosci*, 2011; 34: 611-8.

Jones EG. Thalamocortical dysrhythmia and chronic pain. *Pain*, 2010; 150: 4-5.

Kühn AA, Kempf F, Brücke C, Doyle LG, Martinez-Torres I, Pogosyan A, Trottenberg T, Kupsch A, Schneider G-H, Hariz MI. High-frequency stimulation of the subthalamic nucleus suppresses oscillatory  $\beta$  activity in patients with Parkinson's disease in parallel with improvement in motor performance. *J Neurosci*, 2008; 28: 6165-73.

Kim JH, Chien JH, Liu CC, Lenz FA. Painful cutaneous laser stimuli induce event-related gamma-band activity in the lateral thalamus of humans. *J Neurophysiol*, 2015; 113: 1564-73.

LeBlanc BW, Bowary PM, Chao YC, Lii TR, Saab CY. Electroencephalographic signatures of pain and analgesia in rats. *Pain*, 2016a; 157: 2330-40.

LeBlanc BW, Cross B, Smith KA, Roach C, Xia J, Chao YC, Levitt J, Koyama S, Moore CI, Saab CY. Thalamic bursts down-regulate cortical theta and nociceptive behavior. *Sci Rep*, 2017; 7: 2482.

LeBlanc BW, Lii TR, Huang JJ, Chao YC, Bowary PM, Cross BS, Lee MS, Vera-Portocarrero LP, Saab CY. T-type calcium channel blocker Z944 restores cortical synchrony and thalamocortical connectivity in a rat model of neuropathic pain. *Pain*, 2016b; 157: 255-63.

Leblanc BW, Lii TR, Silverman AE, Alleyne RT, Saab CY. Cortical theta is increased while thalamocortical coherence is decreased in rat models of acute and chronic pain. *Pain*, 2014; 155: 773-82.

Lenz FA, Kwan HC, Dostrovsky JO, Tasker RR. Characteristics of the bursting pattern of action potentials that occurs in the thalamus of patients with central pain. *Brain Res* 1989; 496: 357-60.

Levy R, Deer TR, Henderson J. Intracranial neurostimulation for pain control: A review. *Pain Physician*, 2010; 13: 157-65.

Little S, Pogosyan A, Neal S, Zavala B, Zrinzo L, Hariz M, Foltynie T, Limousin P, Ashkan K, FitzGerald J, Green AL, Aziz TZ, Brown P. Adaptive deep brain stimulation in advanced Parkinson disease. *Ann Neurol*, 2013; 74: 449-57.

Llinas RR, Ribary U, Jeanmonod D, Kronberg E, Mitra PP. Thalamocortical dysrhythmia: A neurological and neuropsychiatric syndrome characterized by magnetoencephalography. *Proc Natl Acad Sci U S A*, 1999; 96: 15222-7.

Luo H, Du X, Huang Y, Green A, Aziz T, Wang S. Dynamic synchronization state identification. 2017 8th International IEEE/EMBS Conference on Neural Engineering (NER), 2017: 525-258.

Mazars GJ. Intermittent stimulation of nucleus ventralis posterolateralis for intractable pain. *Surg Neurol*, 1975; 4: 93-5.

Nguyen JP, Nizard J, Keravel Y, Lefaucheur JP. Invasive brain stimulation for the treatment of neuropathic pain. *Nat Rev Neurol*, 2011; 7: 699-709.

Owen SL, Green AL, Stein JF, Aziz TZ. Deep brain stimulation for the alleviation of

post-stroke neuropathic pain. *Pain*, 2006; 120: 202-6.

Pereira EA, Aziz TZ. Neuropathic pain and deep brain stimulation. *Neurotherapeutics*, 2014; 11: 496-507.

Pereira EAC, Lu GH, Wang SY, Schweder PM, Hyam JA, Stein JF, Paterson DJ, Aziz TZ, Green AL. Ventral periaqueductal grey stimulation alters heart rate variability in humans with chronic pain. *Exp Neurol*, 2010; 223: 574-81.

Priori A, Foffani G, Pesenti A, Tamma F, Bianchi AM, Pellegrini M, Locatelli M, Moxon KA, Villani RM. Rhythm-specific pharmacological modulation of subthalamic activity in Parkinson's disease. *Exp Neurol*, 2004; 189: 369-79.

Putman P, van Peer J, Maimari I, van der Werff S. EEG theta/beta ratio in relation to fear-modulated response-inhibition, attentional control, and affective traits. *Biol Psychol*, 2010; 83: 73-8.

Ray N, Jenkinson N, Kringelbach M, Hansen P, Pereira E, Brittain J, Holland P, Holliday I, Owen S, Stein J. Abnormal thalamocortical dynamics may be altered by deep brain stimulation: using magnetoencephalography to study phantom limb pain. *J Clin Neurosci*, 2009; 16: 32-6.

Rinaldi PC, Young RF, Albefessard D, Chodakiewicz J. Spontaneous neuronal hyperactivity in the medial and intralaminar thalamic nuclei of patients with deafferentation pain. *J Neurosurg*, 1991; 74: 415-21.

Rosenfeld VW, Rutledge DN, Stern JM. Polysomnography with quantitative EEG in patients with and without fibromyalgia. *J Clin Neurophysiol*, 2015; 32: 164-70.

Sarnthein J, Jeanmonod D. High thalamocortical theta coherence in patients with neurogenic pain. *Neuroimage*, 2008; 39: 1910-7.

Sarnthein J, Morel A, von Stein A, Jeanmonod D. Thalamic theta field potentials and EEG: high thalamocortical coherence in patients with neurogenic pain, epilepsy and movement disorders. *Thalamus & Related Systems*, 2003; 2: 231-8.

Sarnthein J, Stern J, Aufferberg C, Rousson V, Jeanmonod D. Increased EEG power and slowed dominant frequency in patients with neurogenic pain. *Brain*, 2006; 129: 55-64.

Schulz E, Tiemann L, Witkovsky V, Schmidt P, Ploner M. Gamma oscillations are involved in the sensorimotor transformation of pain. *J Neurophysiol*, 2012; 108: 1025-31.

Smith HS. Opioids and neuropathic pain. *Pain Physician*, 2012; 15: ES93-110.

Tasker RR. Deep brain stimulation is preferable to thalamotomy for tremor suppression. *Surg Neurol*, 1998; 49: 145-53.

Udupa K, Chen R. The mechanisms of action of deep brain stimulation and ideas for the future development. *Prog Neurobiol*, 2015; 133: 27-49.

van Hecke O, Austin SK, Khan RA, Smith BH, Torrance N. Neuropathic pain in the



general population: a systematic review of epidemiological studies. *Pain*, 2014; 155: 654-62.

Verdonck O, Reed SJ, Hall J, Gotman J, Plourde G. The sensory thalamus and cerebral motor cortex are affected concurrently during induction of anesthesia with propofol: a case series with intracranial electroencephalogram recordings. *Can J Anaesth*, 2014; 61: 254-62.

Wang SY, Aziz TZ, Stein JF, Liu XG. Time-frequency analysis of transient neuromuscular events: dynamic changes in activity of the subthalamic nucleus and forearm muscles related to the intermittent resting tremor. *J Neurosci Meth*, 2005; 145: 151-8.

Wu DL, Wang SY, Stein JF, Aziz TZ, Green AL. Reciprocal interactions between the human thalamus and periaqueductal gray may be important for pain perception. *Exp Brain Res*, 2014; 232: 527-34.

Zhang S, Green A, Smith PP. An automatic classifier of pain scores in chronic pain patients from local field potentials recordings. 2013 6th International IEEE/EMBS Conference on Neural Engineering (NER), 2013: 1194-7.

---

### Highlights

- A segregation approach to screen the quantitative neurophysiological characteristics correlated to pain relief provided by deep brain stimulation.
- An integration model to predict the pain relief provided by deep brain stimulation.
- The pain relief is related to the coherently organized multiple thalamic neural oscillations.